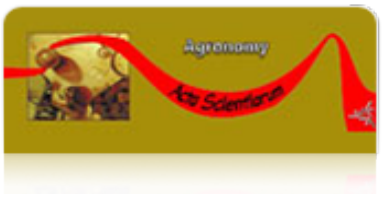


Acta Scientiarum. Agronomy
ISSN: 1679-9275
ISSN: 1807-8621
Editora da Universidade Estadual de Maringá - EDUEM

Soares, Júlia Martins; Medeiros, André Dantas de; Pinheiro, Daniel Teixeira; Rosas, Jorge Tadeu Fim; Silva, Laércio Junio da; Machado, Daniel Lucas Magalhães; Dias, Denise Cunha Fernandes dos Santos

Low-cost system for multispectral image acquisition and its applicability to analysis of the physiological potential of soybean seeds

Acta Scientiarum. Agronomy, vol. 45, e57060, 2023
Editora da Universidade Estadual de Maringá - EDUEM

DOI: https://doi.org/10.4025/actasciagron.v45i1.57060

Available in: https://www.redalyc.org/articulo.oa?id=303075473022

Acta Scientiarum

http://www.periodicos.uem.br/ojs/
ISSN on-line: 1807-8621
Doi: 10.4025/actasciagron.v45i1.57060





# Low-cost system for multispectral image acquisition and its applicability to analysis of the physiological potential of soybean seeds

**Júlia Martins Soares[1], André Dantas de Medeiros[1*], Daniel Teixeira Pinheiro[1], Jorge Tadeu Fim Rosas[2], Laércio Junio da Silva[1], Daniel Lucas Magalhães Machado[3] and Denise Cunha Fernandes dos Santos Dias[1]**

[1]Departamento de Fitotecnia, Universidade Federal de Viçosa, Av. P H Rolfs, s/n, Campus Universitário, 36570-900, Viçosa, Minas Gerais, Brazil. [2]Departamento de Ciência do Solo, Universidade de São Paulo, Piracicaba, São Paulo, Brazil. [3]Syngenta Ltda, Uberlândia, Minas Gerais, Brazil. *Author for correspondence. E-mail: andre.d.medeiros@ufv.br

**ABSTRACT.** The use of multispectral images has great potential to assess seed quality and represents a significant technological advance in the search for fast and non-destructive analysis techniques. However, the devices currently available are expensive. Thus, this study aimed to propose a low-cost method for acquisition and processing of multispectral images of soybean seeds and to evaluate their potential for rapid determination of seed physiological potential. The study was conducted in three steps: implementation of the multispectral image acquisition system, development of an algorithm for automatic image processing, and evaluation of the relationship between the data obtained through image analysis and the results of standard tests used to evaluate seed physiological potential. A total of 43 variables were assessed, eight related to seed physiological potential (germination and vigor) and 35 obtained from the analysis of the multispectral images. Of the variables obtained from multispectral images, 21 were related to pixel values in the images in the different bands evaluated (green, red, and infrared) and 14 associated with seed morphometric characteristics. The proposed system is efficient in obtaining multispectral images and the algorithm developed was efficient to extract morphometric characteristics and pixel information from the images. The parameters obtained from the NIR spectrum region showed a good relationship with the physiological potential of soybean seeds.

**Keywords:** *Glycine max*; seed physiological potential; ImageJ; image processing.

Received on December 12, 2020.
Accepted on May 21, 2021.

## Introduction

Soybean is one of the most important commodities in the world. Currently, almost 349 million tons of grain are produced on approximately 125 million hectares (FAO, 2019). To meet the high demand for soybean grain production, successful establishment of plants in the field is a key factor, which is directly related to the physiological potential of the seeds used (Baek et al., 2019).

Germination test is used for determination of soybean seed quality (Brasil, 2009). The results of this test can be complemented by viability and vigor tests, such as tetrazolium, accelerated aging, and electrical conductivity tests (Krzyananowski, Vieira, & França-Neto, 1999; Brasil, 2009). Although the results of these tests are reliable, they are destructive, time-consuming, and laborious, and must be carried out by well-trained analysts. These characteristics affect the time and the costs involved in carrying out these analyses, considering the large number of seed lots evaluated by seed production companies or in plant breeding programs, which generally evaluate large numbers of genotypes. Thus, fast, accurate, and low-cost methodologies are required for seed quality assessment. Although these methodologies do not replace the standard tests used for the seed trade, they could optimize quality control programs, where the low quality lots could be rapidly eliminated, saving time and resources.

The growing interest in non-destructive and faster strategies for seed quality evaluation has promoted methods based on image analysis. Among the methods available, multispectral imaging has been a promising alternative for detecting fungal contamination, evaluating varietal purity, identifying mechanical damages,

and evaluating components associated with seed development and quality aspects (Boelt et al., 2018). Despite their potential for seed quality assessment, one of the difficulties of implementing techniques that involve multispectral images is the high cost of sensors and equipment, which can restrict their use.

Given the necessity of developing new strategies to assess soybean seed quality, mainly fast and non-destructive approaches, this study aimed to propose a low-cost method using multispectral images acquisition and automatic processing of the soybean seed images. Also, to investigate the relationship between the image parameters and the seed physiological potential.

## Material and methods

### Local and plant material

The study was conducted at the Seed Research Laboratory of the Agronomy Department of the Federal University of Viçosa, in Viçosa, Minas Gerais State, Brazil. Twenty-two (22) soybean seed lots of the cultivar NS6906IPRO, with different levels of physiological potential, were used. The seeds were produced in different commercial areas within the state of Minas Gerais in the crop season of 2018/2019.

### Multispectral imaging system

A low-cost multispectral image acquisition system and image processing workflow was developed. The system was constituted by a camera modified by the Mapir® company (Survey3W model). The camera has the CMOS (Complementary Metal Oxide Semiconductor) sensor Sony Exmor R IMX117 able to register images at a resolution of 12 MP, with a 24-bit pixel depth in the JPEG format and 36-bit in the RAW format. Originally the camera registered RGB (red, green, and blue) images through only a single sensor. The modification of the camera consisted in the removal of a filter that impedes the passage of near-infrared (NIR) light; after removal of this filter, the original Bayer matrix was replaced by a new one. In place of the blue bandpass nano filters, NIR bandpass nano filters were inserted. The images obtained by Survey3W are therefore composed of three bands: R, G, and NIR; and the digital numbers (DN) of these bands correspond to the radiance registered in the electromagnetic spectrum frequency ranges: 643-670 nm, 535-558 nm, and 835-865 nm, respectively.

A structure was set up to acquire the seed images (Figure 1). The camera was placed on a copy stand support at 20 cm from the seed sample. The system was illuminated by halogen lamps (15 watts) that emit a light spectrum in the range of 350 to 2500 nm, which allowed the acquisition of images in the NIR region. During the image acquisition process, the camera focus was fixed in the infinite mode, the ISO at 200, the shutter aperture speed at 1/250 s, and the image format in JPEG. The choice of ISO configurations and shutter aperture speed were determined in a pre-test and the criterion for this choice was the non-existence of saturated pixels in the images considering the three bands.

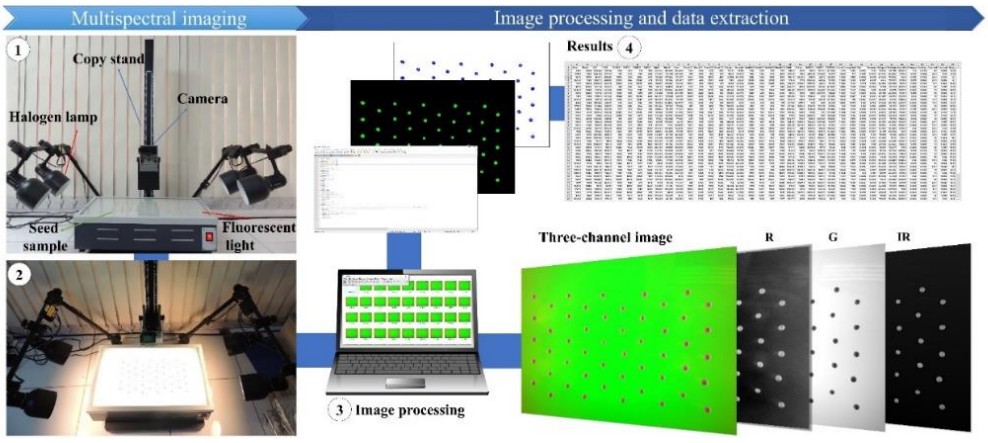


**Figure 1.** System for multispectral image acquisition and image processing. Overview of the equipment for image acquisition (1); sample of seeds placed on the system (2); image segmentation and processing using ImageJ® software (3); and table of results following the analysis (4).

Fluorescent lights placed below the samples were used to enhance the contrast of the seeds in relation to the background to facilitate later segmentation of the image (Figure 1). Images were obtained of 200 seeds from each lot, split into four replications of 50 seeds.

## Image processing

After acquisition, the images were processed through an algorithm in the macro format written in Java programming language on the ImageJ® software. The macro was developed to automatically analyze all the multispectral images simultaneously, generating 21 variables (seven from each band), as well as 14 morphological characteristics of the seeds (Sau, Ucchesu, D'hallewin, & Bacchetta, 2019). In brief, each image was clipped considering the delimitation of the surface of the fluorescent lighting system below the seed sample, and then the images were duplicated. Two functions were developed in the macro. The first consisted of segmentation of the images using the codes HSB (Hue, Saturation, Brightness) of the Color Threshold mode of ImageJ®. The limit of the images was defined with pre-defined values to segment the images in individual regions of interest (in this case, the soybean seeds). A command to execute the plugin Particles8 (https://blog.bham.ac.uk/intellimic/g-landini-software/), used to generate the variables from the images, was inserted in the macro. The second function was developed to create the output images of the seeds identified in the images. The results generated were automatically stored, as well as an image stack containing the original image and the processed image, showing the identification of each seed.

## Physiological analysis

After obtaining the multispectral images, germination and vigor tests were performed. The germination test was conducted on rolls of germination paper (Germitest®) moistened with water in the ratio of 2.5 times the weight of the dry paper, and the rolls were kept in a seed germinator at 25°C for eight days. The percentages of germination were calculated on the fifth day (first germination count) and the eighth day (germination) after the beginning of the test (Brasil, 2009). The number of normal seedlings was counted in these evaluations.

The accelerated aging test was conducted with four replications of 50 seeds per lot, with 220 seeds placed on a stainless-steel screen combined with a *gerbox* (transparent acrylic box for germination) plastic box (11 x 11 x 3.5 cm), containing 40 mL of distilled water. Lids were placed on the boxes and the boxes were kept in a BOD incubator at 41°C for 48 hours. Afterwards, the germination test was performed on the seeds as already described, and the percentage of normal seedlings was determined on the fifth day after the beginning of the test.

The electrical conductivity test was conducted with four replications of 50 seeds. The seeds were initially weighed on an analytical balance with 0.001 g resolution and then placed in plastic cups containing 75 mL of distilled water. The assemblage was kept at 25ºC for 24h. After that period, the electrical conductivity of the solution was determined in a Digimed model DM-32 conductivity meter. The conductivity values were divided by the weight and expressed in $\mu S\ cm^{-1}\ g^{-1}$ of seeds.

A computerized analysis of seedling growth was performed with four replications of 20 seeds. The seeds were distributed in two rows on the upper third of two sheets of paper towel and covered with a third sheet. The paper towel was previously moistened with distilled water in the ratio of 2.5 times the weight of the dry paper. The paper was rolled, put in plastic bags, and placed vertically in a BOD incubator for three days at 25°C. At the end of the period, the seedlings were transferred from the roll of paper to a sheet of blue paperboard with dimensions of 30 × 20 cm. Scanned images were then made and processed individually by the Vigor-S® software (Rodrigues, Gomes-Junior, & Marcos-Filho, 2020), which provided the following variables: hypocotyl length, primary root length, and total seedling length. Also, the growth, uniformity, and vigor indices were calculated.

## Cluster analysis

The data obtained from the tests of the physiological analysis were used for cluster analysis. The Euclidean distance was calculated and the Ward method was applied, with three previously defined groups: high-quality, intermediate-quality, and low-quality seeds. The optimum number of groups was determined by *K-means* method. The clusters formed were characterized regarding seed physiological potential by the germination and vigor tests.

## Statistical analysis

Descriptive analysis of all the data obtained was performed for each cluster. Subsequently, analysis of variance and Pearson correlation ($p < 0.05$) were performed on the data of physiological potential and those obtained through multispectral image analysis. Finally, the principal component analysis was performed using the variables showing significant differences between the clusters. Statistical analyses were performed using the R software (R Core Team, 2019).

# Results

## Performance of the seed lots

In this study, the physiological potential of the 22 soybean seed lots was evaluated using the germination test and four vigor tests. The seed lots showed differences in germination potential, which ranged from 53 to 96% (Figure 2A). The seed lots that did not differ in germination potential exhibited differences in vigor, based on the results of the first germination count (Figure 2B), accelerated aging (Figure 2C), seedling length (Figure 2D), and electrical conductivity (Figure 2E) tests. Thus, the 22 seed lots evaluated exhibited different levels of physiological potential.

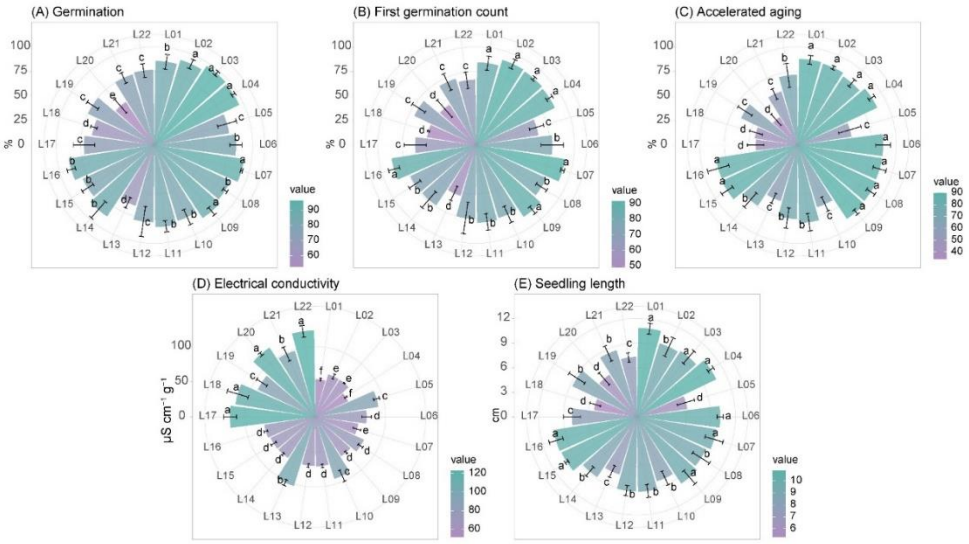


**Figure 2**. Germination and vigor of 22 soybean seed lots showing variability in seed quality.

## Cluster analysis

The data obtained in the seed quality assessment (Figure 2) were used in the cluster analysis. Three groups were formed, based on the performance of the seed lots (Figure 3). The seed lots that exhibited higher percentages of germination and better performance in the vigor tests constituted the first group, which were classified as the high physiological potential group. The second group was constituted by seed lots that had intermediate performance, showing variability in performance, which depended on the vigor test. The second group was therefore classified as having intermediate physiological potential. Seed lots that exhibited lower values of germination and vigor constituted the third group, which were classified as the low physiological potential group. Each group was composed of different numbers of seed lots; the high potential group was composed of six, the intermediate potential group of eight, and the low potential group of eight seed lots.

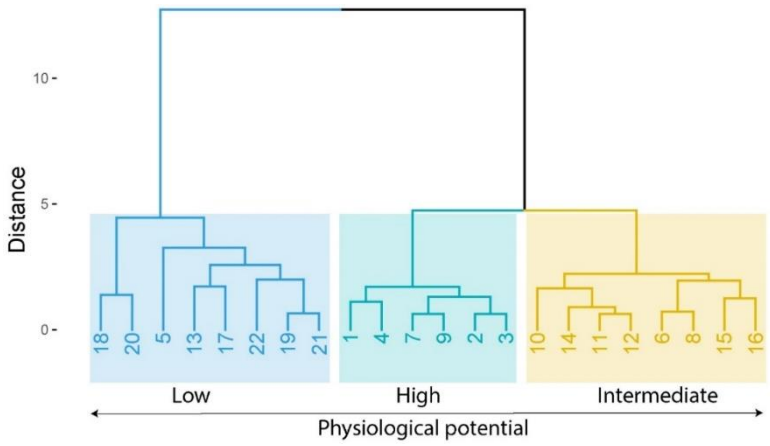


**Figure 3.** Dendrogram of the Euclidean distance of 22 soybean seed lots showing three clusters based on the physiological potential. The clusters were formed based on the germination and vigor data for each lot through the Ward hierarchical method.

## Characterization of each group of seed quality

The groups obtained through cluster analysis (Figure 3) were characterized regarding the physiological potential of the lots. Thus, significant differences ($p < 0.05$) were observed among the groups for most of the parameters evaluated, except for the uniformity index (Table 1). The seed lots that composed the high physiological potential group exhibited germination from 86 to 97%; the intermediate potential group from 79 to 88%; and the low potential group from 53 to 77%. The mean of the parameters related to vigor was greater for the high physiological potential group than the other groups, except for electrical conductivity (Table 1).

**Table 1.** Physiological potential, pixel values of multispectral images and morphological characteristics of soybean seeds clustered based on seed physiological potential.

| Traits | | Physiological potential | | | Prob. > F |
|---|---|---|---|---|---|
| | | High | Intermediate | Low | |
| Physiological analysis | | | | | |
| Germination (%) | | 92[1/] ± 4.13 | 83 ± 3.37 | 69 ± 8.52 | 0.0001 |
| First germination count (%) | | 89 ± 2.65 | 78 ± 4.28 | 61 ± 8.5 | 0.0001 |
| Accelerated aging (%) | | 87 ± 2.27 | 80 ± 7.69 | 54 ± 12.28 | 0.0001 |
| Electrical conductivity (%) | | 60.08 ± 6.07 | 74.53 ± 7.5 | 107.47 ± 13.45 | 0.0001 |
| Seedling length (cm) | | 10.01 ± 0.6 | 9.4 ± 0.74 | 7.18 ± 1.21 | 0.0001 |
| Growth index | | 686 ± 40.68 | 652 ± 62.63 | 493 ± 82.87 | 0.0001 |
| Uniformity index | | 794 ± 40.32 | 745 ± 70.5 | 717 ± 75.91 | 0.402 |
| Vigor index | | 719 ± 39.55 | 680 ± 47.13 | 560 ± 63.29 | 0.0001 |
| Pixel values for each channel | | | | | |
| Infrared | Min | 47.08 ± 0.86 | 45.83 ± 2.55 | 47.08 ± 1.58 | 0.903 |
| (Value Pixels$^{-1}$) | Max | 167.98 ± 2.1 | 171.14 ± 3.24 | 174.66 ± 2.05 | 0.001 |
| | Mode | 119.69 ± 1.35 | 120.33 ± 2.96 | 122.99 ± 1.56 | 0.008 |
| | Median | 119.75 ± 1.32 | 120.58 ± 3.11 | 123.19 ± 1.58 | 0.007 |
| | Average | 119.52 ± 1.29 | 120.66 ± 3.09 | 123.22 ± 1.57 | 0.004 |
| | Skew | -0.7 ± 0.09 | -0.68 ± 0.06 | -0.69 ± 0.06 | 0.799 |
| | Kurt | 1.06 ± 0.19 | 1.16 ± 0.13 | 1.23 ± 0.12 | 0.044 |
| Red | Min | 114.09 ± 0.95 | 112.34 ± 4.27 | 112.45 ± 2.52 | 0.35 |
| (Value Pixels$^{-1}$) | Max | 223.65 ± 1.77 | 225.47 ± 3.33 | 227.54 ± 2.16 | 0.009 |
| | Mode | 159.63 ± 0.79 | 159.54 ± 3.31 | 160.82 ± 1.76 | 0.31 |
| | Median | 164.09 ± 0.77 | 163.83 ± 3.47 | 164.89 ± 1.7 | 0.5 |
| | Average | 167.81 ± 0.77 | 167.72 ± 3.59 | 168.77 ± 1.75 | 0.44 |
| | Skew | 0.41 ± 0.03 | 0.45 ± 0.04 | 0.45 ± 0.04 | 0.05 |
| | Kurt | 0.02 ± 0.04 | 0.06 ± 0.06 | 0.11 ± 0.07 | 0.008 |
| Green | Min | 39.1 ± 2.15 | 37.23 ± 4.09 | 35.82 ± 2.37 | 0.05 |
| (Value Pixels$^{-1}$) | Max | 188.54 ± 1.31 | 189.08 ± 2.58 | 190.43 ± 1.8 | 0.08 |
| | Mode | 56.43 ± 1.94 | 54.84 ± 3.37 | 53.46 ± 2.49 | 0.05 |
| | Median | 76.99 ± 4.03 | 73.37 ± 4.53 | 71.77 ± 2.92 | 0.02 |
| | Average | 84.95 ± 3.26 | 82.07 ± 3.94 | 80.88 ± 2.51 | 0.03 |
| | Skew | 0.89 ± 0.1 | 0.98 ± 0.07 | 1.01 ± 0.05 | 0.006 |
| | Kurt | 0.2 ± 0.23 | 0.44 ± 0.16 | 0.5 ± 0.12 | 0.005 |
| Morphological characteristics | | | | | |
| Perimeter (pixel) | | 219 ± 9.7 | 230 ± 8.18 | 233 ± 3.41 | 0.003 |
| Area (pixel) | | 3396 ± 302.4 | 3721 ± 254.54 | 3816 ± 113.5 | 0.003 |
| Feret | | 70.64 ± 3.18 | 73.87 ± 2.51 | 74.86 ± 1.09 | 0.004 |
| Width | | 62.83 ± 2.61 | 65.76 ± 2.45 | 66.59 ± 1.05 | 0.004 |
| MBCRadius | | 35.36 ± 1.58 | 36.97 ± 1.25 | 37.47 ± 0.54 | 0.003 |
| AspRatio | | 1.12 ± 0.01 | 1.12 ± 0.01 | 1.12 ± 0.01 | 0.91 |
| Circularity | | 0.88 ± 0 | 0.88 ± 0 | 0.88 ± 0 | 0.91 |
| Roundness | | 0.86 ± 0 | 0.87 ± 0.01 | 0.87 ± 0.01 | 0.68 |
| ArEquivD | | 65.5 ± 2.91 | 68.61 ± 2.46 | 69.5 ± 1.02 | 0.003 |
| PerEquivD | | 69.79 ± 3.09 | 73.1 ± 2.6 | 74.05 ± 1.09 | 0.003 |
| Concavity | | 49.04 ± 2.85 | 52.26 ± 2.46 | 53.38 ± 1.26 | 0.002 |
| Shape | | 14.26 ± 0.02 | 14.26 ± 0.02 | 14.26 ± 0.01 | 0.87 |
| ModRatio | | 0.85 ± 0 | 0.86 ± 0.01 | 0.86 ± 0.01 | 0.48 |
| Sphericity | | 0.84 ± 0 | 0.85 ± 0.01 | 0.85 ± 0.01 | 0.39 |

1/ Mean ± standard deviation, n = 6, 8, and 8 seed lots for the high, intermediate, and low physiological potential groups, respectively.

In the analysis of the multispectral images, significant ($p < 0.01$) differences were observed in most variables obtained from the infrared spectrum and in only a minor part of the red and green spectrum (Table 1). The parameters based on the pixel values, namely maximum, mode, median, and average of the multispectral images in the infrared wavelength differed among the groups. Min, kurtosis, and asymmetry, however, did not exhibit significant differences among the groups. The highest values of parameters obtained through multispectral image analysis were observed for the lower physiological potential group. Thus, the greater the germination of the lots, the lower the average obtained for the pixel values of the images in infrared wavelength: 119, 120, and 123 gray pixel$^{-1}$ for the high, medium, and low physiological potential groups, respectively.

In relation to the morphological parameters, significant differences ($p < 0.01$) were observed among the three groups for variables related to seed size and shape (perimeter, area, feret, width, MBCRadius, ArEquivD, PerEquivD, and Concavity) (Table 1). These data show moderate morphological uniformity of the soybean seeds used in this study that were from the same cultivar, but showed small differences related to the seed physiological potential. In general, the low quality seed lots exhibited bigger seeds.

## Principal component analysis

Multivariate principal component analysis was performed using the data obtained for the seed lots in the tests of physiological quality evaluation and from analysis of the multispectral images; i.e., only the variables that showed significant differences among the groups of seed quality were considered in this analysis (Table 1). The central ordering diagram (Figure 4A) shows the arrangement of the 22 individual seed lots, differentiated into their respective groups of physiological potential (high, intermediate, and low). The variables related to the physiological, multispectral, and morphological characteristics of the seeds are presented in the correlation circle (Figure 4B). Although the first two components explained 77% of the total variability of the data, there was a clear separation between the groups, with few points of intersection between the high and intermediate quality groups. Lots in the negative score of PC1 had lower values of germination, accelerated aging, vigor index, and seedling growth, showing, on the other hand, higher values of infrared, red, and green pixel values.

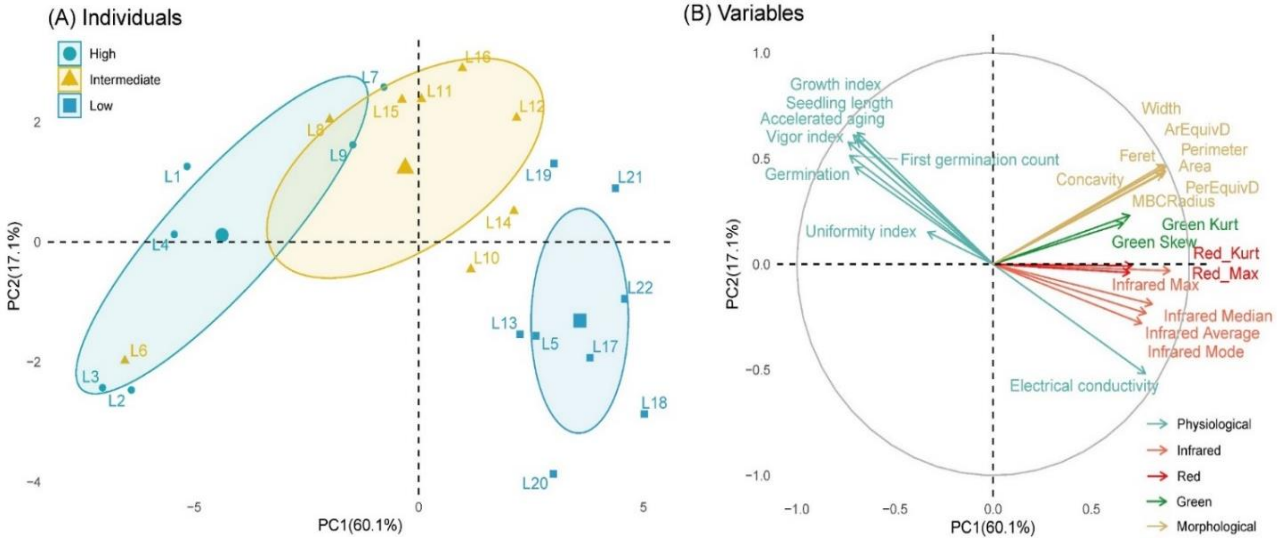


**Figure 4.** Principal component analysis of physiological and infrared variables of 22 soybean seed lots showing variability in the physiological potential. Central ordering diagram of the individuals (A), correlation circle and contribution (B). Ellipses represent confidence interval at 99%.

The correlations among physiological, multispectral, and morphological variables, i.e., among the 43 variables obtained for the seed lots evaluated, are shown in Table 2. In general, the variables indicating seed physiological potential (except seedling uniformity) had negative and significant correlations with most of the variables obtained from the infrared spectrum. Some morphometric variables related to seed size also had significant and inverse correlations with germination, first germination count, and electrical conductivity.

**Table 2.** Correlation coefficients among the physiological parameters and variables extracted from the multispectral images.

| | Germ | FGC | AA | EC | SL | GI | UI | VI |
|---|---|---|---|---|---|---|---|---|
| Infrared | | | | | | | | |
| Min | -0.07 | -0.13 | -0.27 | 0.23 | -0.21 | -0.24 | 0.07 | -0.19 |
| Max | -0.58* | -0.6* | -0.68* | 0.71* | -0.54* | -0.51* | -0.26 | -0.52* |
| Mode | -0.45* | -0.52* | -0.65* | 0.67* | -0.6* | -0.59* | -0.19 | -0.57* |
| Median | -0.45* | -0.52* | -0.65* | 0.66* | -0.58* | -0.57* | -0.19 | -0.55* |
| Average | -0.48* | -0.53* | -0.66* | 0.66* | -0.58* | -0.56* | -0.19 | -0.54* |
| Skew | -0.07 | 0.01 | 0.06 | -0.12* | 0.27* | 0.28* | 0.12 | 0.28* |
| Kurt | -0.3 | -0.38 | -0.38 | 0.49 | -0.52 | -0.51 | -0.32 | -0.53 |
| Red | | | | | | | | |
| Min | 0.19 | 0.12 | -0.04 | -0.04 | -0.05 | -0.07 | 0.1 | -0.03 |
| Max | -0.41 | -0.43* | -0.57* | 0.52* | -0.36 | -0.33 | -0.12 | -0.32 |
| Mode | -0.16 | -0.23 | -0.42 | 0.38 | -0.37 | -0.37 | -0.1 | -0.35 |
| Median | -0.12 | -0.18 | -0.38 | 0.29 | -0.3 | -0.31 | -0.02 | -0.28 |
| Average | -0.14 | -0.19 | -0.39 | 0.29 | -0.3 | -0.3 | -0.01 | -0.27 |
| Skew | -0.23 | -0.23 | -0.24 | 0.27 | -0.1 | -0.08 | -0.09 | -0.1 |
| Kurt | -0.4 | -0.48* | -0.45* | 0.53* | -0.46* | -0.46* | -0.29 | -0.47* |
| Green | | | | | | | | |
| Min | 0.25 | 0.21 | 0.16 | -0.25 | 0.14 | 0.11 | 0.25 | 0.16 |
| Max | -0.33 | -0.35 | -0.51* | 0.43* | -0.3 | -0.29 | -0.03 | -0.27 |
| Mode | 0.25 | 0.21 | 0.18 | -0.27 | 0.17 | 0.14 | 0.24 | 0.18 |
| Median | 0.31 | 0.3 | 0.22 | -0.35 | 0.26 | 0.24 | 0.29 | 0.28 |
| Average | 0.29 | 0.27 | 0.19 | -0.31 | 0.23 | 0.2 | 0.28 | 0.25 |
| Skew | -0.39 | -0.41 | -0.33 | 0.46* | -0.41 | -0.39 | -0.31 | -0.42 |
| Kurt | -0.41 | -0.42 | -0.34 | 0.45* | -0.4 | -0.38 | -0.31 | -0.41 |
| Morphological characteristics | | | | | | | | |
| Perimeter | -0.44* | -0.43* | -0.4 | 0.44* | -0.37 | -0.35 | -0.21 | -0.36 |
| Area | -0.44* | -0.43* | -0.4 | 0.45* | -0.37 | -0.35 | -0.22 | -0.36 |
| Feret | -0.43* | -0.43* | -0.41 | 0.44* | -0.39 | -0.37 | -0.22 | -0.38 |
| Width | -0.45* | -0.43* | -0.39 | 0.45* | -0.35 | -0.32 | -0.19 | -0.33 |
| MBCRadius | -0.44* | -0.43* | -0.41 | 0.44* | -0.39 | -0.37 | -0.22 | -0.38 |
| AspRatio | 0.06 | -0.02 | -0.09 | -0.04 | -0.2 | -0.23 | -0.12 | -0.23 |
| Circularity | -0.03 | 0.05 | 0.03 | 0.06 | 0.13 | 0.15 | 0.09 | 0.15 |
| Roundness | -0.11 | -0.03 | 0.04 | 0.1 | 0.14 | 0.17 | 0.04 | 0.16 |
| ArEquivD | -0.44* | -0.43* | -0.4 | 0.44* | -0.37 | -0.35 | -0.21 | -0.36 |
| PerEquivD | -0.44* | -0.43* | -0.4 | 0.44* | -0.37 | -0.35 | -0.21 | -0.36 |
| Concavity | -0.46* | -0.45* | -0.41 | 0.46* | -0.39 | -0.37 | -0.24 | -0.39 |
| Shape | 0.02 | -0.06 | -0.06 | -0.03 | -0.14 | -0.15 | -0.07 | -0.15 |
| ModRatio | -0.17 | -0.1 | 0.01 | 0.16 | 0.09 | 0.13 | 0.01 | 0.11 |
| Sphericity | -0.19 | -0.12 | -0.01 | 0.18 | 0.08 | 0.12 | 0 | 0.1 |

*significant at 5% by the T test. Legend: Germ = germination; FGC = first germination count; AA = accelerated aging; EC = electrical conductivity; SL= seedling length; GI = growth index; UI = uniformity index; VI = vigor index.

## Discussion

The seed lots used in the present study showed differences in the seed physiological quality (Figure 2). Although all the lots were produced in commercial areas, many factors contribute to the reduction of seed quality in the field, such as rain, high temperatures, diseases, mechanical damage (TeKrony, Egli, & Phillips, 1980; Spears, TeKrony, & Egli, 1997), which leads to the discarding of many soybean seed lots. The pre-harvest deterioration of seeds may occur due to a series of factors that are reflected in biochemical changes, such as the increase in the concentration of ethanol, fatty acids, and changes in lipids and proteins (Bewley & Nonogaki, 2017) following the reduction of seed quality. In this respect, an efficient quality control program is needed, mainly focusing on detecting these alterations.

Using the methodology proposed in this paper, we show that the images generated in the NIR spectral region were efficient in classifying the lots according to level of seed quality (Table 1). The differences in seed physiological potential led to changes in the seed reflectance profile, in which the low physiological potential group exhibited higher pixel values in relation to the intermediate and high potential groups.

Variations in the images obtained in the near-infrared region indicate physical-chemical differences among the seeds that compose the lot (Xia, Xu, Li, Zhang, & Fan, 2019). The radiation from the

electromagnetic region of the near infrared can be absorbed by several compounds contained in the seeds, such as carbohydrates, soluble sugars (Guo et al., 2011), cellulose, hemicellulose, lignin (Huang & Yu, 2019), oil and protein (Agelet & Hurburgh, 2014; Guo et al., 2011), among others. Thus, alterations in these compounds, due to the deterioration process, can be detected by infrared spectrum using NIR spectroscopy (Bazoni, Ida, Barbin, & Kurozawa, 2017). This information is important as it shows the capacity of this spectral region in tracking changes in seed quality, which may be related to differentiated levels of seed deterioration among the seed lots. Previous studies, in which seed lots showing different levels of physiological potential were evaluated, also showed differences in spectral response in the infrared region among the lots (Ambrose, Kandpal, Kim, Lee, & Cho, 2016; Dumont et al., 2015; ElMasry, Mandour, Al-Rejaie, Belin, & Rousseau, 2019; Kusumaningrum et al., 2018).

Thus, our results showed that the analysis of images obtained in the NIR region can be used to infer the soybean seed quality. In this way, low-quality seeds generate images with greater pixel values, and high-quality seeds exhibit low pixel values (Table 1). In future studies, using several seed lots, our methodology could be used to try to establish reference values of pixels for each category of physiological potential.

The seed lots used in the present study were from just one cultivar, but they showed a slight difference in morphometric characteristics of seeds comparing the three groups of seed quality (Table 1). In general, the lots with low quality seeds had bigger seeds, considering mainly the perimeter and area parameters. It is known that these seeds have more propensity to mechanical damage (Moreano et al., 2018), and the damaged seeds are more susceptible to the deterioration process (Neve et al., 2016), which explain the low quality of the seeds of these lots.

Besides the potential of the image analysis, the automation of this process is another contribution of the present work. The macro type code developed in this study was efficient for analyzing several images simultaneously and can be used and adapted for processing multispectral images of seeds using the ImageJ software. Various studies have used this type of tool as a rapid prototyping alternative (Rueden et al., 2017; Schneider, Rasband, & Eliceiri, 2012). The development of customizable macros was also reported as successful for the analysis of tissue integrity and seed morphometry based on digital radiographic images (Medeiros, Silva, Silva, Dias, & Pereira, 2020b).

Technologies that provide faster, less subjective, and precise information about the seed physiological potential are highly desired by seed production companies, in plant breeding programs for soybean seed quality, in seed analysis laboratories, and in the segments linked to soybean production. Recent studies on soybean seeds have shown that technological advances mainly based on image analysis and artificial intelligence algorithms have considerably improved the potential for introducing new technologies in this sector (Baek et al., 2019; Baek et al., 2020; Lin et al., 2019; Mahajan, Mittal, & Das, 2018; Medeiros, Pinheiro, Xavier, Silva, & Dias, 2020a; Zhu et al., 2019).

In this respect, our results provided a promising prospect for the analysis of the physiological potential of soybean seeds through multispectral images with a low-cost system. However, further studies using a greater number of seed lots and seed lots of different cultivars are necessary to validate the practical application of this technique in the routine analysis of soybean seeds. In addition, the combination of multispectral image techniques with modern machine-learning algorithms can be used. This would allow the development of models for individual seed classification regarding the viability or quantitative prediction of the physiological potential of seed lots.

## Conclusion

Multispectral images of soybean seeds were effectively obtained using the proposed methodology. The images were processed in a simple and rapid manner and the macro developed was efficient to extract morphometric characteristics and pixel information from the images. The parameters obtained from the images in the infrared spectrum region showed a relationship with the physiological potential of soybean seed.

## Acknowledgements

The authors are grateful to the Departments of Agronomy and Entomology (UFV, Viçosa, Minas Gerais State, Brazil) for assistance in setting up the experiments; to Syngenta Seeds Ltda. (Brazil) for making seeds available for the study, and for the financial support of the *Fundação de Amparo à Pesquisa do Estado de Minas Gerais* (FAPEMIG) and *Conselho Nacional de Desenvolvimento Científico e Tecnológico* (CNPq). This study was funded in part by the *Coordenação de Aperfeiçoamento de Pessoal de Nível Superior – Brasil* (CAPES) – Finance Code 001.

## References

Agelet, L. E., & Hurburgh, C. R. (2014). Limitations and current applications of Near Infrared Spectroscopy for single seed analysis. *Talanta*, *121*, 288-299. DOI: https://doi.org/10.1016/j.talanta.2013.12.038

Ambrose, A., Kandpal, L. M., Kim, M. S., Lee, W. H., & Cho, B. K. (2016). High speed measurement of corn seed viability using hyperspectral imaging. *Infrared Physics and Technology*, *75*, 173-179. DOI: https://doi.org/10.1016/j.infrared.2015.12.008

Baek, I., Kusumaningrum, D., Kandpal, L. M., Lohumi, S., Mo, C., Kim, M. S., & Cho, B. K. (2019). Rapid measurement of soybean seed viability using kernel-based multispectral image analysis. *Sensors*, *19*(2), 1-16. DOI: https://doi.org/10.3390/s19020271

Baek, J., Lee, E., Kim, N., Kim, S. L., Choi, I., Ji, H., ... Kim, K.-H. H. (2020). High throughput phenotyping for various traits on soybean seeds using image analysis. *Sensors*, *20*(1), 1-9. DOI: https://doi.org/10.3390/s20010248

Bazoni, C. H. V., Ida, E. I., Barbin, D. F., & Kurozawa, L. E. (2017). Near-infrared spectroscopy as a rapid method for evaluation physicochemical changes of stored soybeans. *Journal of Stored Products Research*, *73*, 1-6. DOI: https://doi.org/10.1016/j.jspr.2017.05.003

Bewley, J. D., & Nonogaki, H. (2017). Seed maturation and germination. In *Reference Module in Life Sciences* (p. 623–626). Elsevier. DOI: https://doi.org/10.1016/B978-0-12-809633-8.05092-5

Boelt, B., Shrestha, S., Salimi, Z., Jørgensen, J. R., Nicolaisen, M., & Carstensen, J. M. (2018). Multispectral imaging – a new tool in seed quality assessment? *Seed Science Research*, *28*(3), 222-228. DOI: https://doi.org/10.1017/S0960258518000235

Brasil. (2009). *Regras para análise de sementes*. Brasília, DF: MAPA/ACS.

Dumont, J., Hirvonen, T., Heikkinen, V., Mistretta, M., Granlund, L., Himanen, K., ... Keinänen, M. (2015). Thermal and hyperspectral imaging for Norway spruce (Picea abies) seeds screening. *Computers and Electronics in Agriculture*, *116*(C), 118-124. DOI: https://doi.org/10.1016/j.compag.2015.06.010

ElMasry, G., Mandour, N., Al-Rejaie, S., Belin, E., & Rousseau, D. (2019). Recent applications of multispectral imaging in seed phenotyping and quality monitoring-An overview. *Sensors*, *19*(5), 1-32. DOI: https://doi.org/10.3390/s19051090

Food and Agriculture Organization [FAO]. 2019. *FAOSTAT Food and agriculture data: crops*. Rome, IT: FAO. Retrieved on Nov. 10, 2020 from http://www.fao.org/faostat/en/

Guo, J., You, T., Prisecaru, V., Costescu, D., Nelson, R. L., & Baianu, I. C. (2011). NIR calibrations for soybean seeds and soy food composition analysis total carbohydrates, oil, proteins and water contents. *Nature Precedings*, 1-49. DOI: https://doi.org/10.1038/npre.2011.6611.1

Huang, J., & Yu, C. (2019). Determination of cellulose, hemicellulose and lignin content using near-infrared spectroscopy in flax fiber. *Textile Research Journal*, *89*(23–24), 4875-4883. DOI: https://doi.org/10.1177/0040517519843464

Krzyananowski, F. C., Vieira, R. D., & França-Neto, J. B. (1999). *Vigor de sementes: conceitos e testes*. Londrina, PR: Abrates.

Kusumaningrum, D., Lee, H., Lohumi, S., Mo, C., Kim, M. S., & Cho, B. K. (2018). Non-destructive technique for determining the viability of soybean (*Glycine max*) seeds using FT-NIR spectroscopy. *Journal of the Science of Food and Agriculture*, *98*(5), 1734–1742. DOI: https://doi.org/10.1002/jsfa.8646

Lin, P., Xiaoli, L., Li, D., Jiang, S., Zou, Z., Lu, Q., & Chen, Y. (2019). Rapidly and exactly determining postharvest dry soybean seed quality based on machine vision technology. *Scientific Reports*, *9*(1), 1-11. DOI: https://doi.org/10.1038/s41598-019-53796-w

Mahajan, S., Mittal, S. K., & Das, A. (2018). Machine vision based alternative testing approach for physical purity, viability and vigour testing of soybean seeds (*Glycine max*). *Journal of Food Science and Technology*, *55*, 3949-3959. DOI: https://doi.org/10.1007/s13197-018-3320-x

Medeiros, A. D., Pinheiro, D. T., Xavier, W. A., Silva, L. J., & Dias, D. C. F. S. (2020a). Quality classification of *Jatropha curcas* seeds using radiographic images and machine learning. *Industrial Crops and Products*, *146*, 112162. DOI: https://doi.org/10.1016/j.indcrop.2020.112162

Medeiros, A. D., Silva, L. J., Silva, J. M., Dias, D. C. F. S., & Pereira, M. D. (2020b). IJCropSeed: An open-access tool for high-throughput analysis of crop seed radiographs. *Computers and Electronics in Agriculture*, *175*, 105555. DOI: https://doi.org/10.1016/j.compag.2020.105555

Moreano, T. B., Marques, O. J., Braccini, A. L., Scapim, C. A., França-Neto, J. B., & Krzyzanowski, F. C. (2018). Evolution of the physical and physiological quality of soybean seeds during processing. *Journal of Seed Science*, *40*(3), 313-322. DOI: https://dx.doi.org/10.1590/2317-1545v40n3198414

Neve, J. M. G., Oliveira, J. A., Silva, H. P., Reis, R. G. E., Zuchi, J., & Vieira, A. R. (2016). Quality of soybean seeds with high mechanical damage index after processing and storage. *Revista Brasileira de Engenharia Agrícola e Ambiental*, *20*(11), 1025-1030. DOI: https://dx.doi.org/10.1590/1807-1929/agriambi.v20n11p1025-1030

R Core Team. (2019). *R: A language and environment for statistical computing*. Vienna, AT: R Development Core Team. Retrieved on Nov. 10, 2020 from https://doi.org/http://www.R-project.org

Rodrigues, M., Gomes-Junior, F. G., & Marcos-Filho, J. (2020). Vigor-S: System for automated analysis of soybean seed vigor. *Journal of Seed Science*, *42*, 1-12. DOI: https://doi.org/10.1590/2317-1545v42237490

Rueden, C. T., Schindelin, J., Hiner, M. C., DeZonia, B. E., Walter, A. E., Arena, E. T., & Eliceiri, K. W. (2017). ImageJ2: ImageJ for the next generation of scientific image data. *BMC Bioinformatics*, *18*(1), 1-26. DOI: https://doi.org/10.1186/s12859-017-1934-z

Sau, S., Ucchesu, M., D'hallewin, G., & Bacchetta, G. (2019). Potential use of seed morpho-colourimetric analysis for Sardinian apple cultivar characterisation. *Computers and Electronics in Agriculture*, *162*, 373–379. DOI: https://doi.org/10.1016/j.compag.2019.04.027

Schneider, C. A., Rasband, W. S., & Eliceiri, K. W. (2012). NIH Image to ImageJ: 25 years of image analysis. *Nature Methods*, *9*(7), 671-675. DOI: https://doi.org/10.1038/nmeth.2089

Spears, J. F., TeKrony, D. M., & Egli, D. B. (1997). Temperature during seed filling and soybean seed germination and vigour. *Seed Science & Technology*, *25*(2), 233-244.

TeKrony, D. M., Egli, D. B., & Phillips, A. D. (1980). Effect of field weathering on the viability and vigor of soybean seed. *Agronomy Journal*, *72*(5), 749-753. DOI: https://doi.org/10.2134/agronj1980.00021962007200050014x

Xia, Y., Xu, Y., Li, J., Zhang, C., & Fan, S. (2019). Recent advances in emerging techniques for non-destructive detection of seed viability: A review. *Artificial Intelligence in Agriculture*, *1*, 35-47. DOI: https://doi.org/10.1016/j.aiia.2019.05.001

Zhu, S., Chao, M., Zhang, J., Xu, X., Song, P., Zhang, J., & Huang, Z. (2019). Identification of soybean seed varieties based on hyperspectral imaging technology. *Sensors*, *19*(23), 1-15. DOI: https://doi.org/10.3390/s19235225